Article

Theoretical Study of the Suicide Inhibition Mechanism of the Enzyme Pyruvate Formate Lyase by Methacrylate

Maria de Ftima Lucas, and Maria Joo Ramos

J. Am. Chem. Soc., **2005**, 127 (18), 6902-6909• DOI: 10.1021/ja047699j • Publication Date (Web): 09 April 2005

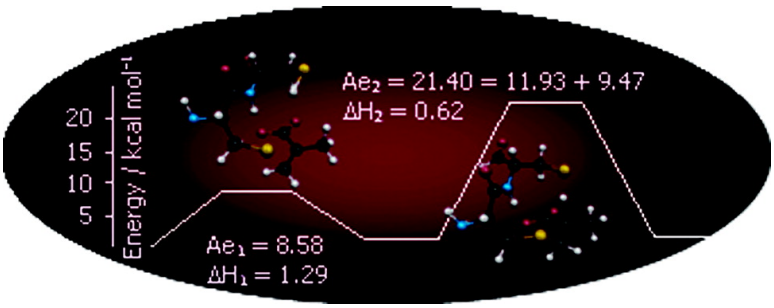

More About This Article

Additional resources and features associated with this article are available within the HTML version:

- Supporting Information
- Links to the 2 articles that cite this article, as of the time of this article download
- Access to high resolution figures
- Links to articles and content related to this article
- Copyright permission to reproduce figures and/or text from this article

View the Full Text HTML

J|A|C|S
ARTICLES
Published on Web 04/09/2005

Theoretical Study of the Suicide Inhibition Mechanism of the Enzyme Pyruvate Formate Lyase by Methacrylate

Maria de Fátima Lucas and Maria João Ramos*

Contribution from REQUIMTE, Departamento de Química, Faculdade de Ciências da Universidade do Porto, Rua do Campo Alegre, 687, 4169-007 Porto, Portugal

Received April 21, 2004; E-mail: mjramos@fc.up.pt

Abstract: The determination of pyruvate formate lyase crystallographic structure brought new insights to its mechanism of reaction and presented the possibility of a direct attack to the substrate from cysteine 418 as opposed to the previously expected cysteine 419. An inhibition study performed by Knappe and co-workers, using substrate-analogue methacrylate, confirms that cysteine 418 is most likely to add directly to pyruvate, since an inhibition product has been found as a substituent in this residue. The work presented here consists of a study of the inhibition mechanism of pyruvate formate lyase by methacrylate, using density functional theory with the hybrid B3LYP functional. We were able to determine all pertinent structures, confirm the proposed experimental mechanism, and add important detail to the energy profile associated with the mechanism of inhibition. Additionally, the obtained results provide the energy values for both the chemical reaction and the stereochemical reorganization necessary in order for the thiol-methacrylate adduct to come within reactional reach of Cys419.

1. Introduction

Pyruvate formate lyase (PFL) replaces pyruvate dehydrogenase in anaerobic conditions during glucose degradation in *Escherichia coli* and other prokaryotes.[1] It is the final enzyme in anaerobic glycolysis in *E. coli*, generating formate and acetylCoA from pyruvate. PFL has been identified as a homodimer of 85 kDa/subunit and is one of the few enzymes that are known to use stable protein-based radicals in their catalytic cycles. Aerobic and anaerobic ribonucleotide reductases (RNRs) are also examples of such enzymes, using tyrosyl and glycyl radicals, respectively, to generate a transient active site thiyl radical, which results in hydrogen atom abstraction in the initial step of RNR reduction. On the other hand, PFL has been shown to require a stable glycyl radical, which results in the rearrangement of pyruvate to formate.

The activation process is catalyzed by an iron(II)-dependent activating enzyme,[2] and it consists of a hydrogen removal from Cα of glycine 734 (Gly734).[2,3] Once in the active form, PFL can function only anaerobically, and exposure to oxygen irreversibly inactivates the enzyme by cleavage of the polypeptide at the glycyl radical site.[4,5]

PFL's catalytic mechanism has been the subject of interest for many years, and it is well established that residues glycine 743 and the two adjacent cysteines 418 and 419 are essential for the enzymatic conversion[1,6−9] of pyruvate and coenzyme A (CoA) into formate and acetyl-CoA. Several mechanisms[9−13] have been proposed from two laboratories: Joachim Knappe and co-workers evidenced in 1974 that the mechanism should take place through ping-pong kinetics,[1] as well as the pioneering proposal of nucleophilic addition from cysteine 418.[10] John Kozarich and collaborators predicted a homolitic process,[12] initiated by a first hydrogen transfer from Gly734 to Cys419. The observation of the crystallographic structure[8] of the enzyme and theoretical studies[14,15] have ruled out some mechanistic possibilities. It is now the consensus that the reaction should take place after a hydrogen transfer from the glycyl radical to cysteine 418 (Cys418), via cysteine 419 (Cys419), followed by addition to pyruvate, which should occur with formyl radical detachment. Initially it was thought that addition to pyruvate should be achieved by Cys419. However, the direct X-ray crystallographic observation of the active site and an inhibition study with methacrylate,[10] a substrate-analogue suicide inhibitor, have ascertained Cys418 as the site for acetylation. The same

* Corresponding author. Tel: +351 22 6082806. Fax: +351 22 6082959.

(1) Knappe, J.; Blaschkowski, H. P.; Gröbner, P.; Schmitt, T. *Eur. J. Biochem.* **1974**, *50*, 253.
(2) Knappe, J.; Schacht, J.; Mockel, W.; Hopner, T.; Vetter, H.; Edenharder, R. *Eur. J. Biochem.* **1969**, *11*, 316.
(3) Conradt, H.; Holman-Berger, M.; Holmann, H. P.; Blaschkowski, H. P.; Knappe, J. *Arch. Biochem. Biophys.* **1988**, *228*, 133.
(4) Reddy, S.; Wong, K.; Parast, C.; Peisach, J.; Magliozzo, R.; Kozarich, J. W. *Biochemistry* **1998**, *37*, 558.
(5) Gauld, J. W.; Eriksson, L. A. *J. Am. Chem. Soc.* **2000**, *122*, 2035.
(6) Wagner, F. V.; Frey, M.; Neugebauer, F. A.; Schäfer. *Proc. Natl. Acad. Sci. U.S.A.* **1992**, *89*, 996.
(7) Knappe, J.; Elbert, S.; Frey, M.; Wagner, F. V. *Biochem. Soc. Trans.* **1993**, *21*, 731.
(8) Becker, A.; Wolf, K.; Kabsch, W.; Knappe, J.; Schultz, S.; Wagner, A. *Nat. Struct. Biol.* **1999**, *6*, 969.
(9) Wong, K. K.; Murray, B. W.; Lewisch, S. A.; Baxter, M. K.; Ridky, T. W.; Ulissi-DeMario, L.; Kozarich, J. W. *Biochemistry* **1993**, *32*, 14102.
(10) Plaga, W.; Vielhaber, G.; Wallach, J.; Knappe, J. *FEBS Lett.* **2000**, *466*, 45.
(11) Plaga, W.; Frank, R.; Knappe, J. *Eur. J. Biochem.* **1988**, *178*, 445.
(12) Parast, C.; Wong, K.; Lewisch, S. A.; Kozarich, J. W. *Biochemistry* **1995**, *34*, 2393.
(13) Leppänen, V.; Merckel, M.; Ollis, D.; Wong, K.; Kozarich, J. W.; Goldman, A. *Structure* **1999**, *7*, 733.
(14) Himo, F.; Eriksson, L. A. *J. Am. Chem. Soc.* **1998**, *120*, 11449.
(15) Lucas, M. F.; Fernandes, P. A.; Eriksson, L. A.; Ramos, M. J. *J. Phys. Chem. B* **2003**, *107*, 5751.

10.1021/ja047699j CCC: $30.25

Scheme 1. Inhibition Mechanism with Methacrylate for the Enzyme Pyruvate Formate Lyase[a]

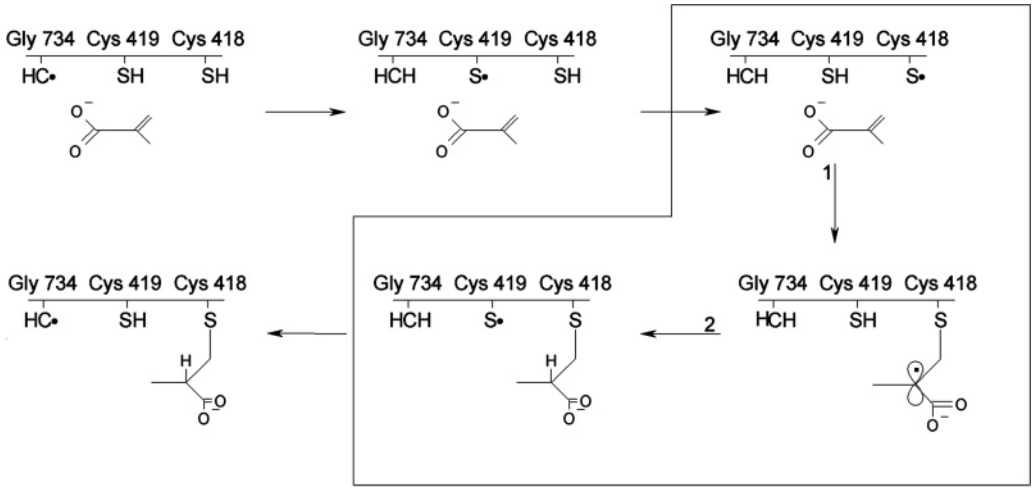

[a] The selected areas corresponding to steps 1 and 2 are different from pyruvate's catalytic mechanism.

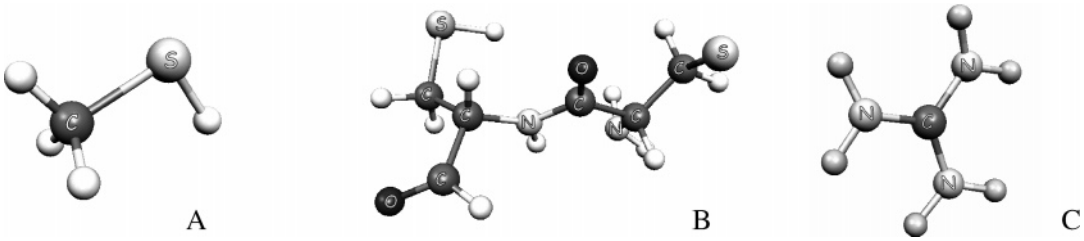

Figure 1. Optimized structures for the models used to represent both cysteines (A and B) and arginines (C): (A) methylthiol; (B) cysteine 419 and cysteine 418 connected by a protein branch; (C) guanidinium ion.

study has reported an energy barrier of 21.40 kcal mol^{-1} for the overall reaction of PFL with methacrylate.

Suicide inhibitors are very important for the study of enzyme mechanisms, as information can be drawn from their interaction with the active site. Their similarity with the natural substrate often leads to an inhibition reaction with the enzyme in an identical manner as the catalytic reaction with the substrate. However, although methacrylate is analogous to pyruvate, we observe that the reaction is quite different and, as opposed to pyruvate, the addition of the thiyl radical occurs exclusively on the C3 methylene carbon. It is expected that the reaction proceeds by hydrogen transfer from Gly734 to Cys418, with Cys419 acting as a bridge between the two residues (Scheme 1). This step of the mechanism is identical to the natural substrate. The difference concerns the thiyl addition. For pyruvate, the reaction takes place at the C2 carbonyl carbon, but it is improbable that the reaction should occur at this position for methacrylate, since the activation energy for the addition on the terminal carbon is 5 kcal mol^{-1} lower than that on the C2 carbon atom. Finally, the reaction proceeds with a hydrogen removal from Cys419, which will in turn abstract a hydrogen atom from the neighboring Gly734, regenerating the radicalar enzyme.

In the course of our studies we observed that the energies that we calculated were within the limits determined experimentally,[10] yet underestimated. To determine the nature of such differences, we have steadily increased our model, first by modeling the two cysteines, 418 and 419, as found in the X-ray crystallographic structure, and later by including also the two arginines, 176 and 435, present in the active site. The two complete cysteines' model made a small difference in the energy barrier, whereas the further inclusion of the two arginines resulted in the same activation energy as observed in their absence.

This made us look back at our results in a different way, and a closer inspection of the X-ray crystallographic structure made us realize that the approximation of the thiol group in Cys419 to methacrylate's C2 carbonyl carbon will only be possible through a reposition of the adduct in the active site, which is in agreement with previous findings.[10] The corresponding stereochemical energy factor can therefore be associated with the difference observed between the experimental activation energy and the calculated barrier, which contains the covalent parcel of the total energy that must be overcome for the reaction to proceed. This enables us to draw some conclusions concerning the fundamental difference of the natural substrate's reaction and the role of the enzyme.

2. Methods

Theoretical calculations are a useful tool for structure prediction and energy barrier determination of enzymatic reactions. In the present work, the active site of the enzyme was represented first by two cysteines (418 and 419) modeled as methylthiol and second as part of the protein branch akin to the crystal structure. Furthermore, we later added to the calculation two arginines which have both been modeled as guanidinium ions. Additionally, we have studied the reaction first with the inhibitor methacrylate represented in its charged form and then as neutral methacrylic acid. All models can be viewed in Figure 1.

All calculations were carried out using the Gaussian 98 quantum chemistry package.[16] The geometries of the stationary points and the energies, for the mechanism under study, were computed using density functional theory (DFT)[17−20] and the hybrid functional B3LYP.[21−23] An unrestricted functional was used given the open-shell nature of all

systems. Geometries were initially optimized using the double-ζ basis set 6-31G(d), and the same basis was used for the calculation of the Hessian (second-derivatives matrix of the energy with respect to nuclear coordinates). Structures are considered optimized if the Hessian has only positive eigenvalues, and transition states were established to have a single imaginary frequency. The Hessian is also used to estimate zero-point, thermal, and entropy effects in the relative energies. The final energies were evaluated performing a single-point calculation using the 6-311+G(3df, 3p) basis set on the previously optimized geometries, with polarized functions added to all atoms and diffuse functions exclusively for heavy atoms. The dielectric effect from the surrounding environment, which accounts for the protein and the buried water molecules, was obtained using the C-PCM polarizable conductor model (Cosmo) developed by Barone and Cossi.[24−27] The dielectric constant was set to 4, which has been shown to be in agreement with experimental results.[28,29]

Intrinsic reaction coordinates[30−32] (IRC) were followed from the transition states toward reactants and products.

Given the radical nature of all systems under study, care must be taken with spin contamination as a possible source of error. Although the DFT wave function is strictly speaking not an eigenfunction of the operator S^2, where S is the electron spin operator, the evaluation of $\langle S^2 \rangle$ still provides a useful control of the quality of the data obtained. In the present work, minor spin contamination occurs for the transition states; however, the value of $\langle S^2 \rangle$ never exceeded 0.773 (ideal value of a pure doublet spin eigenstate is 0.750).

Mulliken population analyses were performed to obtain charge and spin densities, and all energies discussed in this paper are Gibbs energies with solvent effects included.

All complexes illustrated in this work exhibit a large number of minima. The structures discussed in the text are not necessarily the absolute minima but rather the structures that more resemble the geometry of the active site.

3. Results and Discussion

As stated previously, the first two steps of the overall mechanism of inhibition, as well as the last hydrogen transfer from Cys419 to Gly734, have been reported already.[15] Therefore, the present work has concentrated in steps 1 and 2 (Scheme 1), which mainly constitute the inhibition mechanism: thiyl addition to methacrylate and hydrogen transfer from Cys419 to the C2 carbon atom of the Cys418-methacrylate adduct. Both steps have been studied using cysteines 418 and 419 first modeled as methylthiol and later as part of a larger model composed of both these residues as found in the crystallographic structure. The optimized structures of these models can be seen in Figure 1.

Another aspect concerning the models used is related with the fact that, as we are dealing with an anionic system, the use of a neutral model could lead to unrealistic results. Indeed, former studies on PFL[14,15] revealed that the use of a neutral model for pyruvate results in a transition state not observed when the substrate is used in its natural form. Therefore, even though we favor a charged model for methacrylate, we have started our work by analyzing both mechanistic steps with a neutral model vs charged model study, for the sake of finding out whether the model would lead to a different mechanism, just as it happened with pyruvate as the substrate.

3.1. Neutral Model vs Charged Model. We have observed that the use of neutral or charged models does not influence the mechanistic path for the inhibition mechanism of PFL with methacrylate. The optimized structures for both steps of the mechanism with the models (methacrylate and methacrylic acid) employed are shown in Figure 2 and the energetics in Figure 3.

We can observe minor differences in the structures that are, naturally, a consequence of the presence of a hydrogen atom reducing the negative charge in the carboxylate group. The main divergence appears in the energy curve for the second step, where we can see that the neutral system presents a higher activation Gibbs energy barrier. This is to be expected because the extra hydrogen atom in the neutral model causes the spin density in the C2 carbonyl atom to diminish, therefore increasing the activation Gibbs energy barrier for the hydrogen atom transfer from Cys419.

3.2. Thiyl Addition on C2 vs C3. Once in radical form, cysteine 418 is expected to add to methacrylate. The addition to a double bond can occur on either the secondary carbon or the primary carbon. In the present work both possibilities were explored, and we can observe in Figure 4 the optimized structures for addition on the C2 atom.

Observation of Figure 5 and comparison with the energetics for the addition to carbon C3 represented in Figure 3A (step1) shows that although energetically the addition to carbon C2 is possible, the addition to the C3 atom on the other hand takes place with a lower activation Gibbs energy barrier (7.08 vs 2.07 kcal mol^{-1}, respectively).

Given this situation, it is unlikely that an equilibrium should get established and only reaction with carbon C3 is expected to occur. This leaves out the possibility of a similar path as its analogue pyruvate.

3.3. Thiyl Addition to Methacrylate. A Larger Cys-Cys Model. The studies presented so far have been carried out with the two cysteines represented as methylthiols. To differentiate the two cysteines present in the mechanism, a larger model that contains both residues connected by the protein backbone has also been used to complete this study. The optimized structures for thiyl nucleophilic addition, observed in Figure 6, show that structural differences are insignificant compared to the methylthiol model (Figure 2A, step1).

We can observe that the distance separating the thiyl group in this system is larger than that for the small methylthiol group.

(16) Frisch, M. J.; Trucks, G. W.; Schlegel, H. B.; Scuseria, G. E.; Robb, M. A.; Cheeseman, J. R.; Zakrzewski, V. G.; Montgomery, J. A., Jr.; Stratmann, R. E.; Burant, J. C.; Dapprich, S.; Millam, J. M.; Daniels, A. D.; Kudin, K. N.; Strain, M. C.; Farkas, O.; Tomasi, J.; Barone, V.; Cossi, M.; Cammi, R.; Mennucci, B.; Pomelli, C.; Adamo, C.; Clifford, S.; Ochterski, J.; Petersson, G. A.; Ayala, P. Y.; Cui, Q.; Morokuma, K.; Malick, D. K.; Rabuck, A. D.; Raghavachari, K.; Foresman, J. B.; Cioslowski, J.; Ortiz, J. V.; Stefanov, B. B.; Liu, G.; Liashenko, A.; Piskorz, P.; Komaromi, I.; Gomperts, R.; Martin, R. L.; Fox, D. J.; Keith, T.; Al-Laham, M. A.; Peng, C. Y.; Nanayakkara, A.; Gonzalez, C.; Challacombe, M.; Gill, P. M. W.; Johnson, B. G.; Chen, W.; Wong, M. W.; Andres, J. L.; Head-Gordon, M.; Replogle, E. S.; Pople, J. A. *Gaussian 98*, revision A.3; Gaussian, Inc.: Pittsburgh, PA, 1998.
(17) Thomas, L. H. *Proc. Cambridge Philos. Soc*. **1927**, *23*, 542.
(18) Fermi, E. *Acad. Naz. Linzei*. **1927**, *6*, 602.
(19) Slater, J. C. *Phys. Rev*. **1951**, *81*, 385.
(20) Hohenberg, P.; Kohn, W. *Phys. Rev*. **1964**, *136*, 864.
(21) Becke, A. D. *J. Chem. Phys*. **1993**, *98*, 1372.
(22) Becke, A. D. *J. Chem. Phys*. **1993**, *98*, 5648.
(23) Lee, C.; Yang, W.; Parr, R. G. *Phys. Rev. B* **1988**, *37*, 785.
(24) Barone, V.; Cossi, M.; Tomasi, J. *J. Chem. Phys*. **1997**, *107*, 3210.
(25) Miertus, S.; Scrocco, E.; Tomasi, J. *J. Chem. Phys*. **1981**, *55*, 117.
(26) Tomasi, J.; Bonaccorsi, R.; Cammi, R.; Valle, F. J. O. *J. Mol. Struct. (THEOCHEM)* **1991**, *234*, 401.
(27) Tomasi, J.; Bonaccorsi, R. *Croat. Chem. Acta* **1992**, *65*, 29.
(28) Blomberg, M. R. A.; Siegbahn, P. E. M.; Babcock, G. T. *J. Am. Chem. Soc.* **1998**, *120*, 8812.
(29) Siegbahn, P. M. E.; Eriksson, L. A.; Pavlov, M. *J. Phys. Chem. B* **1998**, *102*, 10622.
(30) Gonzalez, C.; Schlegel, H. B. *J. Chem. Phys*. **1989**, *90*, 2154.
(31) Gonzalez, C.; Schlegel, H. B. *J. Phys. Chem*. **1990**, *94*, 5523.
(32) Truhlar, D. G.; Kupperman, A. *J. Am. Chem. Soc*. **1971**, *93*, 1840.

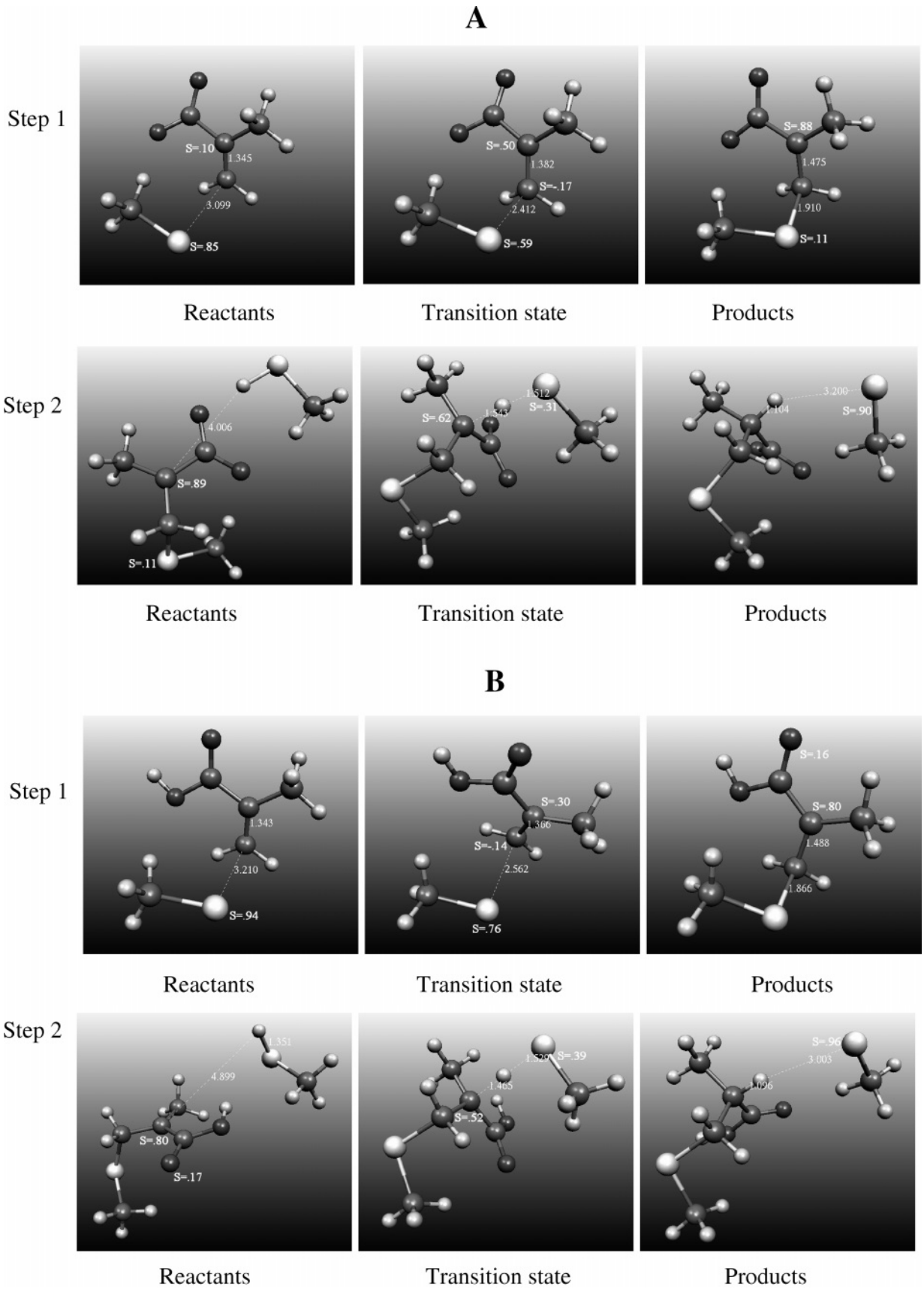

Figure 2. Optimized geometries for the inhibition mechanism using (A) methacrylate and (B) methacrylic acid.

This explains the higher activation Gibbs energy barrier (8.58 kcal mol^{-1}) compared to the smaller model (Figure 3A). Although an increase is observed in the activation energy for this larger model, it is still quite low considering the reported activation barrier for this mechanism, which makes it unfeasible for this process to be the rate-limiting step. On the other hand,

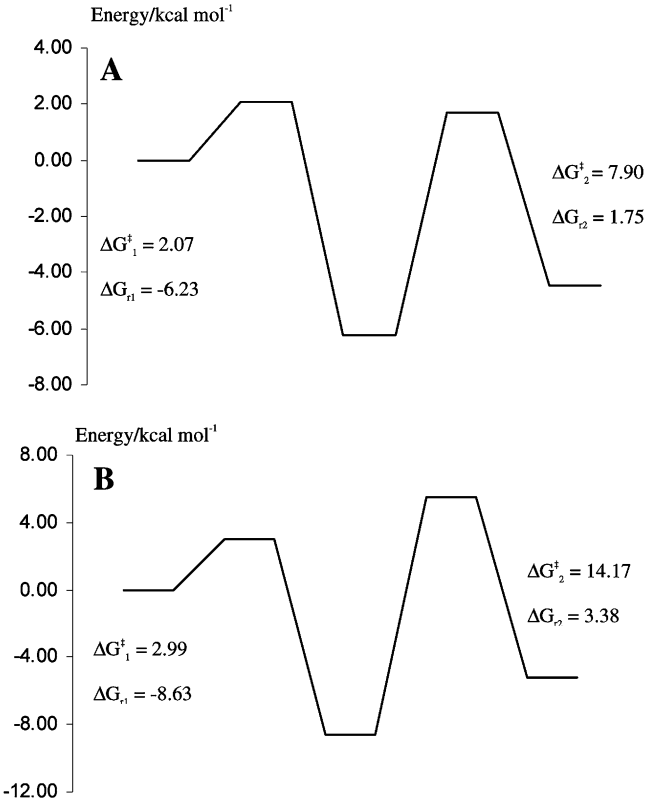

Figure 3. Schematic energy surface for (A) methacrylate and (B) methacrylic acid. $\Delta G^{\ddagger}$ stands for activation Gibbs energy, and ΔG_r stands for reaction Gibbs energy.

the observation of both transition states (small and large model) illustrate that all pertinent distances are alike and that no significant differences in geometries are observed. The products are also similar, although in this model the C−S bond is slightly shorter than that for the small model. It can also be seen that the product contains a radical located on carbon C2, which will complete its valence by removing a hydrogen atom from the neighboring cysteine 419. The calculated spin densities diverge slightly in the reactants and transition state when proceeding from the small to the larger model. The spin density on the sulfur atom calculated for the small model reactants is 0.85 opposed to 0.96 of the larger model. Likewise, the transition state for the methylthiol system shows a value of 0.59 for the same atom, while on the larger system the equivalent atom presents a 0.62 spin density.

3.4. Hydrogen Removal from Cysteine 419. Small Cys Model vs Larger Cys-Cys Model. Once the addition is concluded, it is expected that the radical intermediate should remove a hydrogen atom from C419. The reaction is accompanied by a 7.9 kcal mol^{-1} activation Gibbs energy barrier using the smaller methylthiol model, and a slightly higher barrier of 11.9 kcal mol^{-1}, when the two cysteines are included as found in the crystallographic structure. We can see in Figure 7 that the C−H distance in the reactants is identical to the corresponding one in the small model (Figure 2A, step 2). The transition state exhibits a distance of 1.520 Å for C−H and 1.525 Å for S−H, and the equivalent distances in the small model are 1.543 and 1.512 Å, respectively, which shows that minor structural differences are observed. For the products we can see that 5.445 Å separates the sulfur atom on cysteine 419 from the extracted hydrogen, while in the small model this distance is only 3.200 Å.

An Even Larger Model with the Inclusion of Arg176 and Arg435. At this point we were confronted with the fact that although this barrier (11.93 kcal mol^{-1}) is nearer to the experimental value (21.40 kcal mol^{-1}), it is still low, and in order to determine if the model used was adequate, two more residues were introduced and the transition state was located in the presence of the two arginines 176 and 435 (Figure 8B). The results (an activation Gibbs energy barrier of 7.6 kcal mol^{-1} compared to 7.9 kcal mol^{-1} in the absence of the arginines) confirm that the positively charged residues do not influence the magnitude of the activation barrier. Given the simple nature of the process, another route of inhibition is not expected. The difference of 9.47 kcal mol^{-1} in the energy between the experimental and the calculated values must arise therefore from another source, which we set out to investigate. (To ascertain that the difference between the experimental and the calculated values was not caused by the use[33,34] of the B3LYP functional or/and the corresponding BSSE errors, we have performed single-point calculations for all structures at the B97-2/6-311+G(3df,3p) level,[35] with continuum. We have also calculated the counterpoise corrections for all the small models. However, albeit interesting, these newly calculated values do not alter the resulting mechanism or the conclusions withdrawn with the B3LYP calculations. They have been included in Supporting Information.)

3.5. Inside the Enzyme. Figure 9A shows the active center of PFL with pyruvate, just as it can be observed in the X-ray crystallographic structure.[8] Figure 8B shows the active site of PFL into which we have docked methacrylate. This we have done painlessly by direct substitution over pyruvate, due to the likeness of the two species.

We can see from Figure 9 that for the first step of the reaction (thiyl addition) the species pyruvate and methacrylate must overcome a distance of 2.562 and 2.956 Å, respectively. There is a slight increase in distance for the second species; however, the thiyl addition from Cys418 to methacrylate takes place on a terminal carbon that has a certain degree of freedom and can easily position itself in the most convenient place. On the other hand, the second step for pyruvate's reaction consists of a hydrogen removal from Cys419 by the formyl radical. This group is free to move in the active site. However, the same does not happen with methacrylate. There is no group detachment, and the reaction consists of a hydrogen transfer from Cys419 to the C2 carbon atom of the adduct, where there is a

(33) Lynch, B. J.; Truhlar, D. G. *J. Phys. Chem. A* **2001**, *105*, 2936.
(34) Zhao, Y.; Pu, J.; Lynch, B. J.; Truhlar, D. G. *Phys. Chem. Chem. Phys.* **2004**, *6*, 673
(35) Frisch, M. J.; Trucks, G. W.; Schlegel, H. B.; Scuseria, G. E.; Robb, M. A.; Cheeseman, J. R.; Montgomery, J. A., Jr.; Vreven, T.; Kudin, K. N.; Burant, J. C.; Millam, J. M.; Iyengar, S. S.; Tomasi, J.; Barone, V.; Mennucci, B.; Cossi, M.; Scalmani, G.; Rega, N.; Petersson, G. A.; Nakatsuji, H.; Hada, M.; Ehara, M.; Toyota, K.; Fukuda, R.; Hasegawa, J.; Ishida, M.; Nakajima, T.; Honda, Y.; Kitao, O.; Nakai, H.; Klene, M.; Li, X.; Knox, J. E.; Hratchian, H. P.; Cross, J. B.; Adamo, C.; Jaramillo, J.; Gomperts, R.; Stratmann, R. E.; Yazyev, O.; Austin, A. J.; Cammi, R.; Pomelli, C.; Ochterski, J. W.; Ayala, P. Y.; Morokuma, K.; Voth, G. A.; Salvador, P.; Dannenberg, J. J.; Zakrzewski, V. G.; Dapprich, S.; Daniels, A. D.; Strain, M. C.; Farkas, O.; Malick, D. K.; Rabuck, A. D.; Raghavachari, K.; Foresman, J. B.; Ortiz, J. V.; Cui, Q.; Baboul, A. G.; Clifford, S.; Cioslowski, J.; Stefanov, B. B.; Liu, G.; Liashenko, A.; Piskorz, P.; Komaromi, I.; Martin, R. L.; Fox, D. J.; Keith, T.; Al-Laham, M. A.; Peng, C. Y.; Nanayakkara, A.; Challacombe, M.; Gill, P. M. W.; Johnson, B.; Chen, W.; Wong, M. W.; Gonzalez, C.; Pople, J. A. *Gaussian 03*, revision B.04; Gaussian, Inc.: Pittsburgh, PA, 2003.

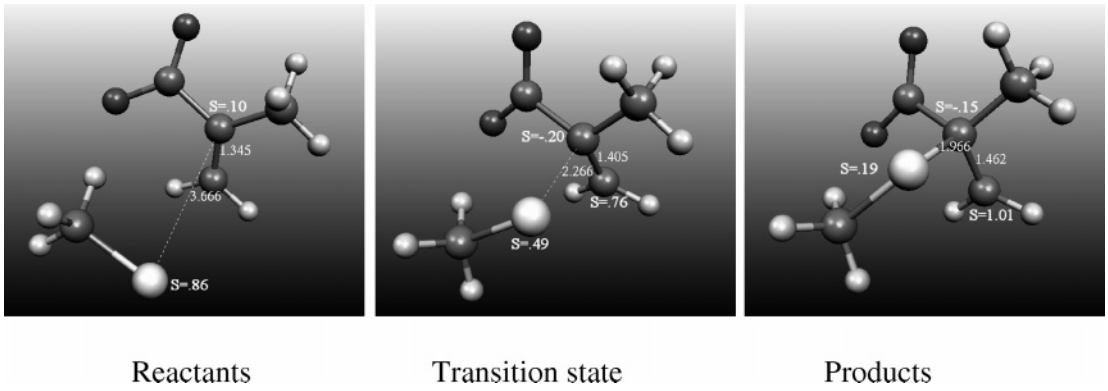

Figure 4. Optimized geometries for the addition of thiyl radical to C2 on methacrylate.

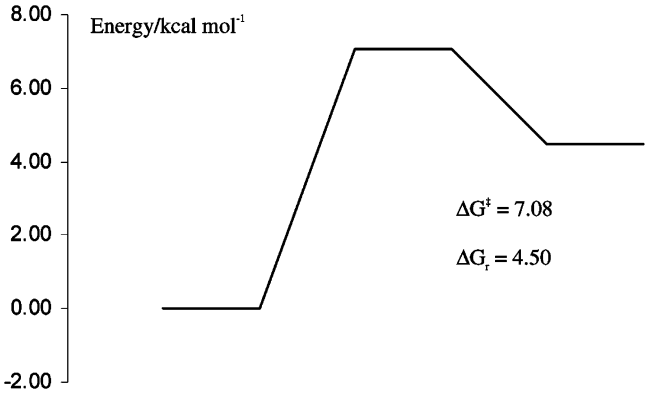

Figure 5. Schematic energy surface for thiyl addition to C2 on methacrylate. $\Delta G^{\ddagger}$ stands for activation Gibbs energy, and ΔG_r stands for reaction Gibbs energy.

large distance barrier that has to be surmounted. There is clearly a difference between the positions of the two species in the active site of PFL, which basically translates into a repositioning of the adduct before the abstraction of the hydrogen atom from methacrylate is made possible. All this points in the direction of attributing the energy difference between the calculated and experimental values to the rearrangement of the active site, necessary for the reaction to proceed. Furthermore, the structural modifications that take place in the active site of the enzyme are responsible for the slower reaction. Therefore this must be the rate-limiting step. Additionally, we are encouraged to believe that once the necessary modifications occur, it is not possible to restore the active site to its original form, which explains the irreversible inhibition of methacrylate.

4. Conclusions

The work presented here is another step in the slow process of understanding the behavior of PFL. This enzyme belongs to a group of radical enzymes such as class III anaerobic ribonucleotide reductase or benzylsuccinate synthase, and the

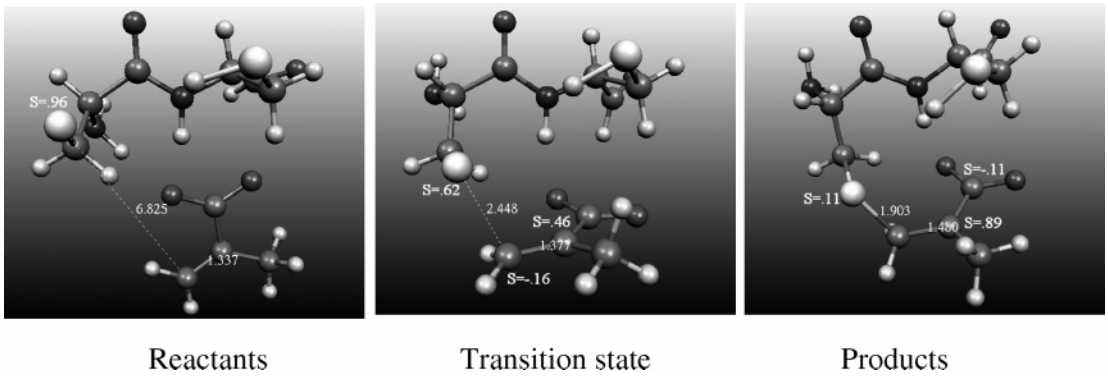

Figure 6. Optimized structures and calculated Mulliken spin densities for thiyl addition of methacrylate to carbon C3 using the larger model containing both cysteines.

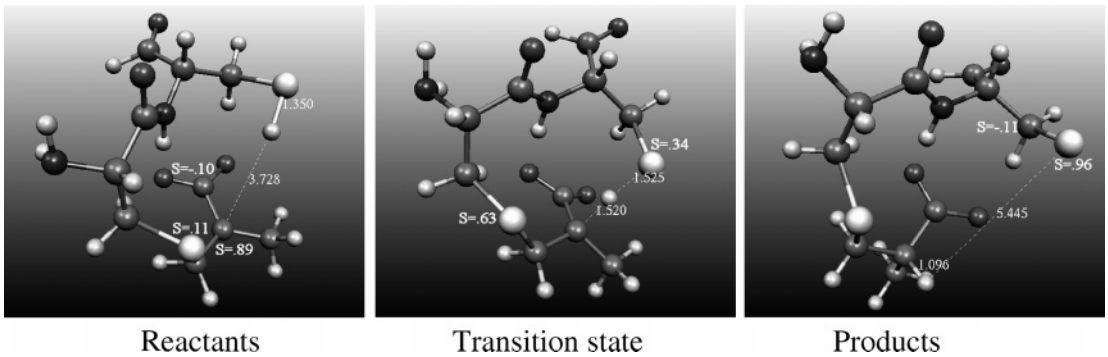

Figure 7. Optimized structures and calculated Mulliken spin densities for hydrogen abstraction on the C2 atom by the C418-methacrylate adduct.

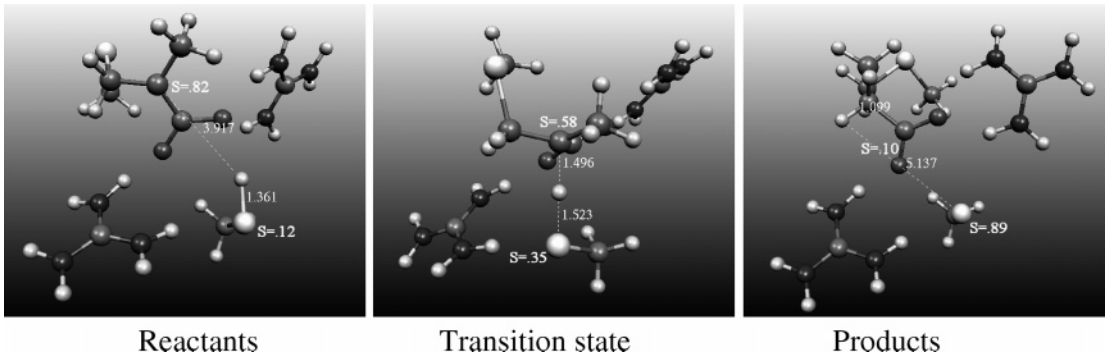

Figure 8. Optimized structures and calculated Mulliken spin densities for hydrogen abstraction on the C2 atom by the C418-methacrylate adduct in the presence of the two arginines 176 and 435.

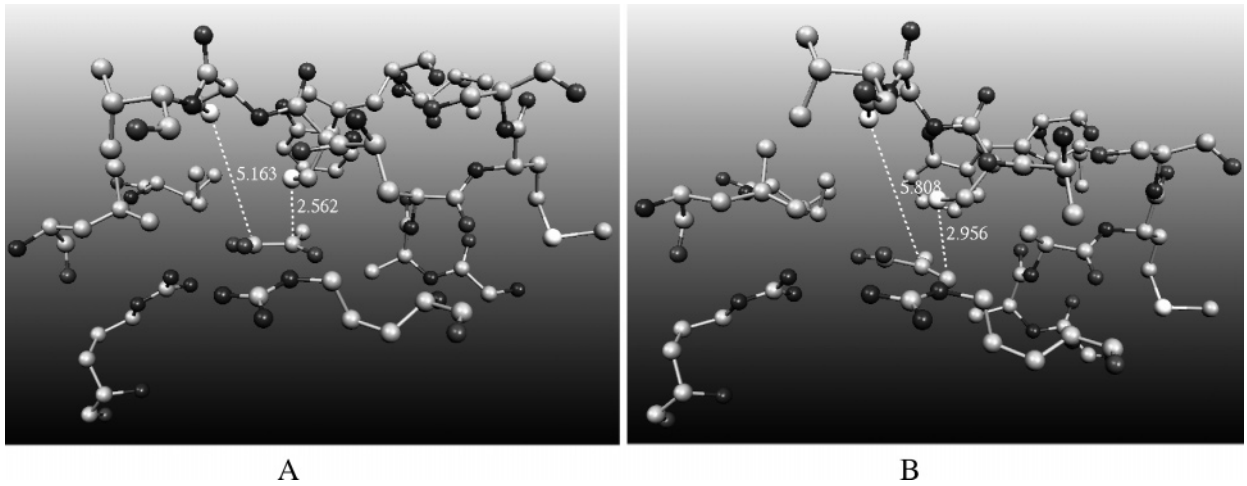

Figure 9. Active site of PFL as obtained by X-ray crystallography:[8] (A) with pyruvate and (B)[8] with modeled methacrylate.

comprehension of PFL's mechanism is important given the biological significance of these enzymes. Another interesting feature of this enzyme is the use of thiyl groups through the conversion of pyruvate into formate. However, the existence of two adjacent cysteines in the active center complicated the direct function assignment of these residues. Only upon observation of the crystal structure of PFL in complex with its natural substrate was it possible to scrutinize that both cysteines were in position to have an active part in the reaction. In addition to this information, the study of inactivation by methacrylate evidenced that cysteine 418 could be responsible for the direct addition on pyruvate.

Using the DFT functional B3LYP we have evaluated the PFL inhibition mechanism with methacrylate and have validated the path established by means of experimental results. The mechanism is initiated by a hydrogen transfer to Cys418 from Gly734 via Cys419 and differs from the natural substrate in two steps: the thiyl addition is achieved on the terminal carbon C3 as opposed to pyruvate, which adds to the C2 carbonyl carbon, and the hydrogen transfer takes place from C419 to carbon C2.

The potential energy surface in terms of Gibbs energies is shown in Figure 10.

The overall process presents a small energy gain of 1.9 kcal mol^{-1}. It has been established that, in this particular case, the use of a neutral or charged model does not influence the mechanistic path.

It was observed that addition of thiyl 418 to carbon C2 is within the limits imposed by the experimental results. However,

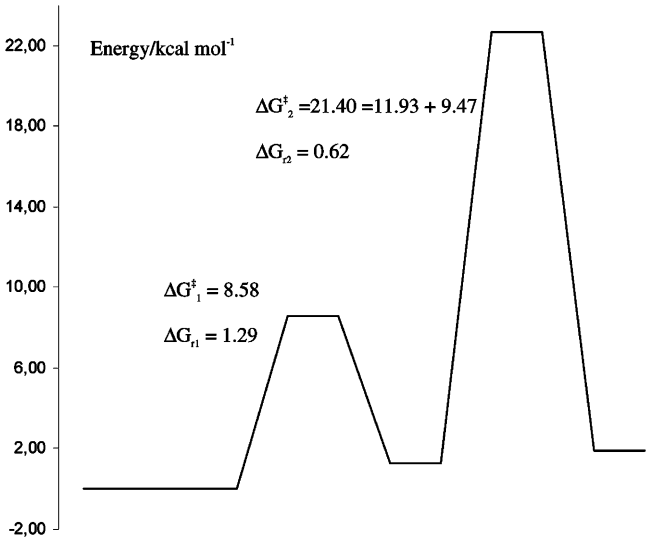

Figure 10. Calculated overall energies for PFL inhibition mechanism by methacrylate. $\Delta G^{\ddagger}$ stands for activation Gibbs energy, and ΔG_r stands for reaction Gibbs energy.

the barrier is 5 kcal mol^{-1} higher than the corresponding addition to carbon C3. Consequently, we do not expect that an equilibrium occurs, and therefore, the reaction must take place exclusively at the methylene carbon C3.

The calculated energy barriers determine the hydrogen transfer from Cys419 to methacrylate as being the slowest

process and, therefore, the rate-limiting process. On the basis of the calculated energy results and the experimental kinetic data and on close observation of the active center of the enzyme, we were able to attribute the value of 9.47 kcal mol^{-1} to the chemical reaction, which occurs in the rate-limiting process, and the value of 11.93 kcal mol^{-1} to the stereochemical reorganization of the active site during this step. Additionally, we believe that these modifications necessary for the reaction to proceed are responsible for the irreversibility of the reaction.

Acknowledgment. The Fundação para a Ciência e Tecnologia (Project POCTI/35736/99, Portugal, and a Ph.D. grant for M.F.L.) is gratefully acknowledged.

Supporting Information Available: Single point calculations for all structures at the B97-2/6-311+G(3df,3p) level, with continuum. Counterpoise corrections for all the small models. This material is available free of charge via the Internet at http://pubs.acs.org.

JA047699J